Extracellular Matrix Targeted MRI Probes

Giuseppe Digilio, Sara Lacerda, Begoña Lavin Plaza, Alkystis Phinikaridou

Concept
doi.org/10.1002/anse.202200039

Chemistry Europe
European Chemical Societies Publishing

www.analysis-sensing.org

Extracellular Matrix Targeted MRI Probes

Giuseppe Digilio[+],[b] Sara Lacerda[+],[c] Begoña Lavin Plaza,[d] and Alkystis Phinikaridou*[a]

Dysregulated remodeling of the extracellular matrix (ECM) can lead to excessive accumulation of ECM proteins (primarily collagen, elastin/ tropoelastin, fibronectin and fibrin) resulting in tissue fibrosis. In many pathologies, changes in the molecular pattern of ECM components have been related to the progression and severity of fibrosis. Thus, magnetic resonance imaging (MRI) probes sensing specific ECM components hold promise for accurate staging of fibrotic diseases. This paper focuses on gadolinium-based contrast agents (GBCA) targeted to ECM components, including structural proteins and enzymes. According to available examples, they can be grouped into: 1) GBCA conjugated to targeting vectors that recognize and non-covalently bind to specific sites on the molecular target; 2) GBCA carrying a reactive chemical function able to bind covalently to the complementary chemical function of the molecular target; and 3) enzyme-responsive probes, whose relaxivity and pharmacokinetics change after enzymatic processing. Pros and cons of each approach are discussed.

1. Introduction

1.1. Scale of the problem

Fibrosis is part of a natural wound healing process that follows injury to any tissue, characterized by the accumulation of extracellular matrix (ECM) proteins primarily collagens, elastin/ tropoelastin, fibronectin and fibrin.[1] If excessive, however, fibrosis can lead to scarring resulting in organ damage and/ or failure responsible for ~45% of all deaths in the industrialized world.[2] Fibrosis is key in cardiovascular, liver, lung, kidney, cancer and other diseases.[1,3] Methods to quantify the extent of fibrosis and stage disease are still largely based on an invasive biopsy. This, however, is not always possible and is not without risk.

[a] *Dr. A. Phinikaridou*
Department of Biomedical Engineering
King's College London
School of Biomedical Engineering and Imaging Sciences
Westminster Bridge Road, SE1 7EH, London (UK)
E-mail: alkystis.1.phinikaridou@kcl.ac.uk
[b] *Dr. G. Digilio[+]*
Department of Science and Technological Innovation
Università del Piemonte Orientale "Amedeo Avogadro"
Viale T. Michel 11, 15121 Alessandria (Italy)
[c] *Dr. S. Lacerda[+]*
Centre de Biophysique Moléculaire, CNRS, UPR 4301
Université d'Orléans
Rue Charles Sadron, 45071 Orléans Cedex 2 (France)
[d] *Dr. B. Lavin Plaza*
Department of Biochemistry and Molecular Biology
School of Chemistry
Complutense University
Ciudad Universitaria s/n, 28040 Madrid (Spain)
[+] *These authors contributed equally to this manuscript.*

1.2. Current limitations of existing imaging approaches

Despite advancements in understanding the mechanisms of fibrosis and innovations in imaging technologies, two major challenges still exist. Firstly, clinically available noninvasive imaging modalities such as MRI, computed tomography (CT) and ultrasound (US) have been used to assess fibrosis by evaluation of its functional consequences (e.g., tissue stiffness) or by providing surrogate measures (e.g., the tissue extracellular volume, T_1 and T_2 relaxation times by MRI).[4,5] However, both functional consequences and surrogate markers provide only indirect measures of fibrosis that can be affected by factors unrelated to fibrosis (i.e., inflammation, edema), thus may be considered unspecific, and also they have not always been validated against biopsy. Secondly, clinically available imaging methods do not provide direct quantification of changes in ECM proteins or enzymes involved in ECM turnover. This hampers accurate staging of disease and monitoring the effectiveness of treatments.

1.3. Solution

Molecular imaging, using targeted probes, has emerged as a potential solution to overcome the limitations of current imaging approaches. Molecular imaging probes may allow direct, quantitative and selective assessment of ECM proteins and enzymes involved in ECM turnover within tissues in order to detect and stage fibrosis accurately, noninvasively and safely.[6] Such tools could have large implications in preclinical research, clinical diagnosis, and drug trials. In this Concept article, we explore the opportunities and challenges for developing, testing, and validating MRI molecular probes targeted to ECM components.

2. Opportunities

2.1. Biology of ECM proteins

Fibrillar types I and III collagens are abundant in the interstitial matrix, making up 80–90% of the collagen in the body.[7] Fibrillar collagen is secreted as procollagen and undergoes modification, cleavage, and crosslinking by lysyl oxidase (LOX), to form mature collagen fibrils. Similarly, elastin is abundant in the arterial wall contributing to 50% of its dry weight.[8] Mature elastin is an insoluble and hydrophobic polymer, formed by LOX-induced enzymatic crosslinking of its soluble precursor monomer, tropoelastin.[9] Impaired collagen and elastin biosynthesis, ineffective or excessive crosslinking and/or degradation by matrix metalloproteinases (MMPs) drive multiple diseases. Another multifunctional adhesive ECM glycoprotein with key roles in tissue repair is fibronectin, that is overexpressed for example, in cancer.[10–12] Finally, tissue injury may also trigger the coagulation cascade, resulting in the formation of fibrin (intravascular or extravascular). Fibrin is an insoluble protein formed by enzymatic polymerization of fibrinogen catalyzed by thrombin.[13] Excessive production of fibrin leads to thrombosis whereas ineffective production or premature lysis of fibrin may lead to haemorrhage.

2.2. Molecular Imaging of ECM components

2.2.1. Choice of imaging modality

Because of the central role of ECM components in diseases, ECM proteins and enzymes involved in ECM turnover (namely MMPs) have been used as imaging and therapeutic targets. Molecular imaging enables direct quantification of biological processes that underpin different stages of diseases by detecting and/or responding to specific biomarkers (e.g., deregulated proteins/receptors, or parameters such as pH, pO_2, temperature).[14] Targeted probes usually comprise a metal chelate (imaging reporter) conjugated to a vector unit, via a linker. Vectors can be small molecules, peptides, aptamers, or antibodies that recognize a specific protein/receptor, or cell type. Most imaging modalities can utilize molecular probes, and choosing the appropriate modality depends on the local concentration of the target within the tissue and the resolution of the image required. For example, positron emission tomography (PET) and single-photon emission computed tomography (SPECT) can detect very low concentrations of the target (pM-nM) allowing imaging of most biological targets, and PET can provide absolute quantification. However, PET and SPECT have lower spatial resolution than MRI, require a radiochemistry facility near the imaging centre, and involve ionizing radiation, which makes these techniques less practical for following patients over time. MRI provides much higher resolution and additional anatomic and functional information but has lower

Giuseppe Digilio is an Assistant Professor in Chemistry at the University of Eastern Piedmont "A. Avogadro", Italy. In 1998 he received his PhD in Protein Chemistry from the University of Turin, Italy. From 1999 to 2007 he was appointed as Head of the Chemistry Lab at Bioindustry Park del Canavese (Italy), a science park focused on biotechnology and pharmaceutical research. His current research interests include the chemistry of molecular probes, with emphasis on the design, synthesis, characterization and validation of molecular and microenvironment-responsive probes for MR and multimodal imaging.

Sara Lacerda received her PhD from the University of Lisboa (2009), during which she developed and studied in vitro and in vivo theranostic agents. Later, she did a short postdoc at the University of Lübeck, Germany, on Fragment-Based Drug Discovery. In 2010–2012, her research focused on bimodal Optical/MRI lanthanide-based lipo-nanoparticle contrast agents, at Centre de Biophysique Moléculaire (CBM), Orléans, France. From 2013–2015, she worked as Research Associate at KCL's Imaging Sciences Division, London, UK, on new PET/MRI targeted probes for cardiovascular diseases. In 2016, she re-joined CBM as a CNRS Researcher. Her current project focuses on multimodal peptide-based contrast agents.

Begoña Lavin-Plaza is a Lecturer in the Department of Biochemistry and Molecular Biology at the Complutense University of Madrid, Spain. She received her PhD in Biology from the Spanish National Center for Cardiovascular Research - Alcalá University, Madrid, Spain in 2013. From 2013–2020 she worked as Research Associate in the School of Biomedical Engineering and Imaging Sciences at King's College London, UK. Her research focuses on enhancing the understanding of the molecular mechanisms underpinning the role of vascular inflammation on different cardiovascular diseases and identifying new biomarkers that can be used as therapeutics and/or imaging probes.

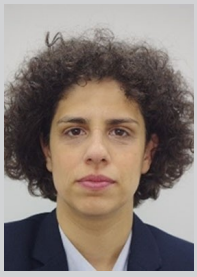

Alkystis Phinikaridou is a Senior Lecturer in Imaging Biology at King's College London. She has received her Ph.D. in Physiology from Boston University, MA, USA in 2009. Her research focuses on developing and applying novel MRI and PET imaging agents and non-invasive MRI imaging protocols to stage disease in experimental models of cardiovascular diseases. Specific areas of interest include imaging of extracellular matrix proteins (elastin/tropoelastin and collagen), endothelial permeability and inflammation. She has also successfully translated preclinical findings into patients, bridging the clinical translational gap.

sensitivity (μM-mM) requiring higher injected dose of the contrast agent or the design of highly efficient or "smart" contrast agents.

2.2.2 Characteristics of a good MRI agent

This concept paper focuses on T_1 relaxation agents promising for molecular imaging of fibrosis. These agents are mostly gadolinium-based contrast agents (GBCAs), but chelates and nanoparticles of Mn(II) and Fe(III) are attracting growing interest. The ideal fibrosis agent should exhibit:

1) High binding affinity to the target protein (low equilibrium dissociation constant - K_d) and high binding specificity (low nonspecific binding to other ECM proteins or components).
2) Fast clearance of the unbound fraction from both the circulation and the diseased tissue (low background signal).
3) High relaxivity to enhance MRI contrast using the lowest injected dose. The ability of a T_1 relaxation agent to generate MRI contrast is described in quantitative terms by its relaxivity (r_1), defined as the enhancement of the water proton relaxation rate promoted by the agent at 1 mM concentration. The relaxivity is expressed in units of $mM^{-1}s^{-1}$. The higher the relaxivity, the higher is the ability of a contrast agent to enhance image contrast. Higher relaxivity agents result in MRI signal amplification and can provide equivalent contrast enhancement at a lower dose compared with low relaxivity agents. The relaxivity of a given relaxation agent depends on many factors, including magnetic field strength, temperature, pH, ionic strength and the solution rotational dynamics of the complex. Some low molecular weight Gd(III)-complexes may gain a higher relaxivity when they bind to their protein target because the rotational dynamics of the complex are slowed down (this is known as the "macromolecule effect").[15–17] A relaxivity gain after target recognition (e.g., by exploiting the macromolecule effect) should be pursued whenever possible to maximize sensitivity.
4) Good safety profile to facilitate clinical translation. Considering the low sensitivity of MRI and the higher injected dose required, the metal chelate must be kinetically inert - thus preventing in vivo release of toxic metal ions. The current trend is to develop GBCA based on macrocyclic chelates, such as DOTA (1,4,7,10-tetraazacyclododecane-1,4,7,10-tetraacetic acid), as they have better kinetic stability in respect to linear chelates such as DTPA (diethylenetriamine pentaacetic acid).[18] Additionally, probes should be excreted soon after imaging; they must not inhibit or activate any other biological processes, such as an immune response, and should not interact with other therapeutic agents.
5) A linear relationship between tissue accumulation and imaging signal is desirable to enable quantification of the target. Unlike other techniques (e.g., nuclear medicine), quantification of the target by MRI is a very challenging task. The problem of quantification stems from the fact that the observed MR signal has contributions both from the free and the target-bound forms of the probe. As mentioned above, the relaxivity of the bound probe can be appreciably different from that of the free probe. Without exact knowledge of the relaxivity of the bound form, and without independent knowledge of the total concentration of the probe in the tissue, it is then impossible to assess the mixing ratio between the free and the bound form of the probe, hence to quantify the target. A very elegant solution of this problem is given by the T_2/T_1 ratiometric approach, that is based on the measurement of T_2 and T_1 parametric maps (an example of this approach as applied to MMP-activity imaging is given at the end of Section 3.2). However, the currently used parametric mapping techniques (e.g., T_1 and T_2 mapping) depend on specifics of the MRI system hardware, pulse sequence implementation, physiological variables (e.g., blood pressure and heart rate) and are susceptible to respiratory and cardiac motion resulting in potentially inaccurate and misleading data. To overcome these limitations, magnetic resonance fingerprinting (MRF) approaches have been proposed[19] to simultaneously map multiple properties such as T_1 and T_2 relaxation times in a single scan with the potential to yield reproducible measurements of tissue properties independent of scanner, software and physiological variables. Thus, MRF could help overcome the so-called MRI signal quantification problem.[20,21]

3. State of the Art

Three main strategies have been used to design fibrosis-related imaging probes (Figure 1):

1) GBCA conjugated to a targeting vector (e.g., a small molecule or peptide) that recognize and non-covalently bind to specific sites on the molecular target. To improve sensitivity, multimeric/ dendrimeric Gd(III)-complexes or paramagnetic nanoparticles (e.g., liposomes, micelles) can be used.
2) GBCA carrying a reactive chemical function able to form a covalent bond with a complementary chemical function of the molecular target.
3) GBCA conjugated to a substrate of the target enzyme, whose relaxivity and pharmacokinetics are changed after enzymatic processing (enzyme-responsive probes).

3.1. MRI probes to image ECM proteins

3.1.1. Elastin/ tropoelastin

The targeting vector approach has been used for imaging of total tissue elastin (Gd-ESMA),[22–31] and the precursor molecule tropoelastin (Gd-TESMA).[32–34] These agents consist either of a peptidomimetic or peptide targeting moiety linked to a Gd(III)-complex. Gd-ESMA was initially developed using the DTPA chelator, but to facilitate clinical translation the DTPA was later replaced by a DOTA derivative. For the same reason, Gd-TESMA was originally developed using the DO3AAm chelator. Gd-

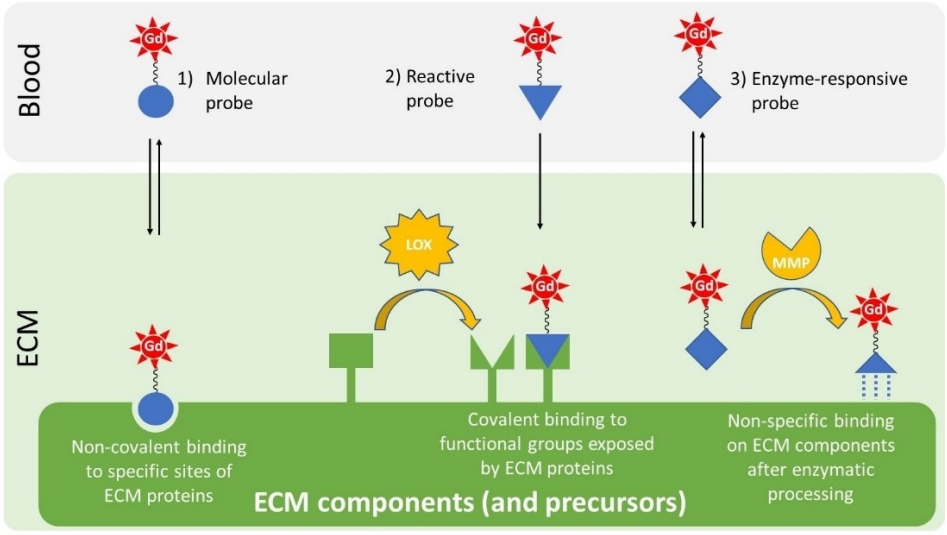

Figure 1. Strategies for molecular imaging of structural components and enzymes in the extracellular matrix.

ESMA was shown to bind equally to both crosslinked elastin and tropoelastin but with higher affinity towards crosslinked elastin. Conversely, Gd-TESMA was designed to bind to monomeric tropoelastin but not to crosslinked elastin.[32] Both agents showed favorable pharmacokinetics in vivo (blood clearance within 1 h post-injection) and exhibited increased relaxivity upon binding to the target.

Up to date, molecular imaging using Gd-ESMA has enabled measurement of total elastin-related fibrosis in preclinical models of cardiovascular, renal, and liver disease.[22–31] Signal enhancement following Gd-ESMA was shown to peak at 30 minutes, but persisted up to 2 h post-injection allowing sufficient time for imaging. Gd-ESMA enabled noninvasive quantification of atherosclerotic plaque size and reduction of disease in statin-treated mice.[23] Gd-ESMA also provided a noninvasive tool to detect positive vessel wall remodeling enabling detection of high-risk/unstable atherosclerotic plaques that cause thrombotic events in a rabbit model.[25] Importantly, Gd-ESMA also allowed detection of coronary disease by quantifying plaque burden and stent-induced vascular remodeling in pigs.[26,27] This is promising for diagnosis of coronary disease that underpins acute coronary syndromes in man. Finally, Gd-ESMA allowed a clear delineation and assessment of myocardial scar size in mice.[28,29]

Active, yet incomplete, elastogenesis and elastolysis favor the accumulation of tropoelastin within tissue.[35] Therefore, tropoelastin may provide a more disease-specific biomarker than mature elastin. Molecular imaging using Gd-TESMA abrogated the signal coming from endogenously present, crosslinked, elastin in the vessel wall and enabled selective detection of tropoelastin, indicative of dysfunctional elastogenesis in atherosclerotic plaques and aortic aneurysms in mice.[32,33] The signal from Gd-TESMA was reduced in statin-treated atherosclerotic mice allowing monitoring of treatment response. Interestingly, changes in plaque relaxation rate (R_1) after injection of Gd-TESMA provided a more sensitive biomarker for detecting high-risk plaques in a rabbit model compared with Gd-ESMA[32] (Figure 2).

Despite the promising results using Gd-TESMA, signal enhancement peaked at 30 minutes post-injection limiting imaging to ~1 h. To overcome this challenge, the tetrameric Gd_4-TESMA agent was developed by replacing the single Gd-DO3AAm unit with a small $[Gd\text{-}DO3AAm]_4$ unit. This modification increased the relaxivity per molecule by ~4-fold.[34] The tetrameric Gd_4-TESMA increased the contrast-to-noise ratio between the plaque and blood (by 6-fold) and doubled the imaging time-window (to 2 h) to study atherosclerosis in mice.[34] This approach may facilitate imaging of tissues requiring longer scans and/or higher signal (e.g., for imaging the coronary arteries).

3.1.2. Collagen and fibrogenesis

A peptide-based agent incorporating three Gd-DTPA moieties for signal enhancement has been developed as a type I collagen-specific probe (EP-3533).[36] *In vivo* biodistribution studies in mice showed fast clearance from blood and higher uptake in organs with naturally higher collagen content (e.g., liver, heart, kidneys, lungs). Imaging with EP-3533 demonstrated clear delineation and significant enhancement of myocardial scar;[36] enabled detection and staging of liver[37,38] and lung[39] fibrosis; muscular dystrophy;[40] pancreatic cancer[41] and quantification of the response to anti-fibrotic therapy[42] in mice. Changes in MRI signal after injection of EP-3533 correlated with collagen content determined by measurements of hydroxyproline. As discussed above, to facilitate clinical translation of the EP-3533, an improved probe – CM-101 – was conjugated to three Gd-DOTA-like moieties (namely, DOTAGA).[43] Compared with EP-3533, CM-101 showed decreased blood half-life, and lower retention in the liver, bone, and kidneys. CM-101-enhanced MRI was observed in fibrotic

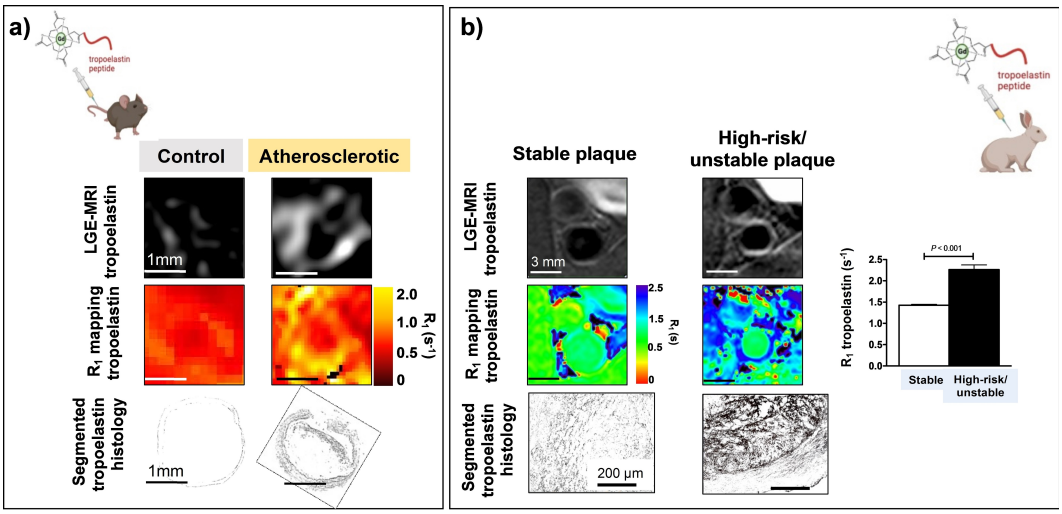

Figure 2. Tropoelastin imaging with the Gd-TESMA probe. The agent enables imaging of dysfunctional elastogenesis in atherosclerotic mice (a) and detection of high-risk/ unstable plaque in rabbits (b). LGE = Late Gadolinium Enhancement. *Reproduced from* Ref. .[32] *Copyright (2018), with permission from Wolters Kluwer Health, Inc.*

livers and correlated with hydroxyproline and collagen content.[44]

Unlike the previous examples, in the ProCA32 probe Gd(III) is directly coordinated by the amino acid residues of a peptide sequence that was specifically designed to yield high thermodynamic stability.[45] This Gd(III)-binding peptide was then conjugated to a collagen type I targeting peptide to generate the ProCA32.collagen1 probe. Further PEGylation improved the relaxivities and increased both blood stability and tissue retention time.[46] ProCA32.collagen1 has been used as a dual T_1/T_2 probe. *In vivo* MRI enabled detection of alcohol-induced liver fibrosis and early-stage non-alcoholic steatohepatitis. The detected MRI signal correlated with histological and elemental Gd tissue analyses.

To improve sensitivity when imaging ECM proteins, targeted nanoparticles and micelles that increase local Gd-payload have also been developed. For example, high-density lipoprotein (HDL)-based nanoparticles conjugated with EP-3533 and Gd-chelates[47] enhanced the in vivo MR signal in aortic walls of atherosclerotic mice in the plaque regression group (by ~82 %) compared with the progression group. *Ex vivo* studies showed that nanoparticles co-localized with collagen. Finally, a bimodal fluorescence/MRI micellar system decorated with the CNA35 protein that binds to several collagen types (I, III and IV)[48] was successfully used to image collagen remodeling in mice with aortic aneurysm[49] and atherosclerosis.[50]

A second strategy to image fibrosis is by reactive agents that bind covalently to the complementary reactive groups of the target. Agents such as Gd-Hyd, Gd-OA, and Gd-CHyd target reactive aldehydes present on allysine residues that are precursors of crosslinked collagen. The Gd-Hyd molecule has a reactive hydrazine moiety that selectively binds to allysine, with very low nonspecific binding to other proteins, resulting in a 5 minute blood half-life in mice.[51] Gd-Hyd MRI enabled detection of active fibrogenesis (versus stable scar) in lung and liver fibrosis.[51] The time course of MRI signal changes paralleled the tissues' LOX activity and total allysine content. Despite the benefits of the fast blood clearance of Gd-Hyd in reducing background signal, these kinetics also limit the time that the complex is exposed to the target tissue. For this reason, an improved allysine-targeted probe, Gd-CHyd, was developed in which the reactive hydrazine moiety was switched to alkyl hydrazine.[52] This substitution resulted in an 11-fold increase in the aldehyde binding rate constant and an order of magnitude higher affinity for aldehydes leading to a higher MRI signal of fibrotic lungs.[52] Another modification of the Gd-Hyd probe involved substitution of the hydrazide by an oxyamine group to generate the Gd-OA probe.[53] Gd-OA was shown to bind to allysine with a higher affinity and r_1 bound relaxivity than Gd-Hyd. Gd-OA resulted in stronger MRI signal in fibrotic lungs which was abrogated by decreasing the amount of allysine using a LOX inhibitor.

3.1.3. Fibronectin

Both small probes and nanoparticles were explored to visualize fibronectin/fibrinogen. A promising small aptamer-based T_1/T_2 agent showed an unexpected hypertense T_2-signal enhancement in human blood clot phantoms, while the T_1-signal was increased in whole blood preparations because of the presence of fibrinogen.[54] Gd-CLT1 (decapeptide) enabled enhancement of colon tumours in mice despite having rather low r_1/r_2 relaxivities.[55] The second generation of the agent (with replacement of DTPA with a DOTA analogue and conjugation on a nanoglobule surface) showed improved relaxivity and renal excretion of the unbound agent, enabling detection of the stroma of prostate tumours in mice.[56] The shorter pentapeptide tetrameric-agent based on DOTA-monoamide like chelate, CREKA-dL-$(Gd\text{-}DOTA)_4$, revealed strong enhancement in prostate tumours within 5 minutes post-injection[57] and its tripod analogue enabled robust contrast

enhancement of metastatic breast tumours and detection of micro-metastases (< 0.5 mm), extending the detection limit of the current clinical imaging modalities despite having a slightly lower r_1 relaxivity (Figure 3).[58] Finally, the high relaxivity CREKA-dL-(Gd-AAZTA)$_4$ tetrameric probe based on the AAZTA chelator (6-amino-6-methylperhydro-1,4-diazepinetetraacetic acid)[59] enabled detection of prostate cancer with a reduced dose of injected gadolinium.[60]

The Fibronectin Extra-Domain B (EDB) based-probe (MT218) showed tumour enhancement that lasted for 30 minutes post-injection in a breast cancer model and in small pancreatic tumours allowing for accurate tumour delineation (even at low 0.02 mmol Gd/kg dose).[61,62] Importantly, detection of pancreatic ductal adenocarcinoma metastasis was possible at low doses.[63] Finally, nanoparticles decorated with EDB-specific aptides and Gd-DTPA provided strong MRI signal enhancement of atherosclerotic plaques in mice that was validated ex vivo using cyanine-labelled analogues.[64]

3.1.4. Fibrin

Another example of a peptide-based tetrameric Gd agent is the fibrin-binding probe, initially developed using the DTPA chelator (EP-1873)[65] which was later replaced by DOTAGA (EP-2104R).[66] This agent allowed successful detection of thrombi and intraplaque fibrin in experimental models.[67,68] EP-2104R is among the few MR targeted agents that have reached clinical trials, showing selective enhancement of atrial and ventricular thrombi, deep venous thrombosis, and carotid artery thrombus in patients.[69,70] A version of the fibrin-binding peptide EP-2104R bearing a tetrameric, high relaxivity Gd(III)-AAZTA complex has been reported, but no in vivo data are available.[71]

3.2 MRI probes to image ECM enzymes

ECM enzymes that may have high value to diagnose fibrosis are MMP, LOX and myeloperoxidase (MPO). MPO is a ubiquitous extracellular biomarker of inflammation. Examples of MPO MR imaging in preclinical models of cardiovascular inflammation and lung fibrosis have been recently reviewed.[72] LOX has a key role in the formation of mature, crosslinked ECM components and its activity was shown to be altered in cardiovascular diseases, in fibrosis-related pathologies, and in cancer. Several examples of molecular imaging probes either containing LOX activatable groups or targeted to LOX-derived allysine/aldheyde groups are available for nuclear or optical imaging (OI) modalities.[73] LOX activity can be followed only indirectly by MRI through molecular probes that bind to allysine residues of collagen and elastin (see section 3.1.2).

The human MMP family includes 23 members of endoproteases that have a key role in ECM turnover.[74] Besides ECM degradation, MMPs have many regulatory functions, including the processing of chemokines, cytokines, growth factors, and activation of other MMPs. As a result, an individual MMP can trigger a complex spectrum of events in vivo, eliciting a response that is highly tissue and pathology specific. According to the context, each MMP can have either anti-fibrotic or pro-fibrotic functions.[75,76] For these reasons, there have been several attempts for in vivo molecular imaging of MMPs, using either MMP inhibitors or substrates. The inhibitor approach relies on imaging-labelled inhibitors that after selective binding

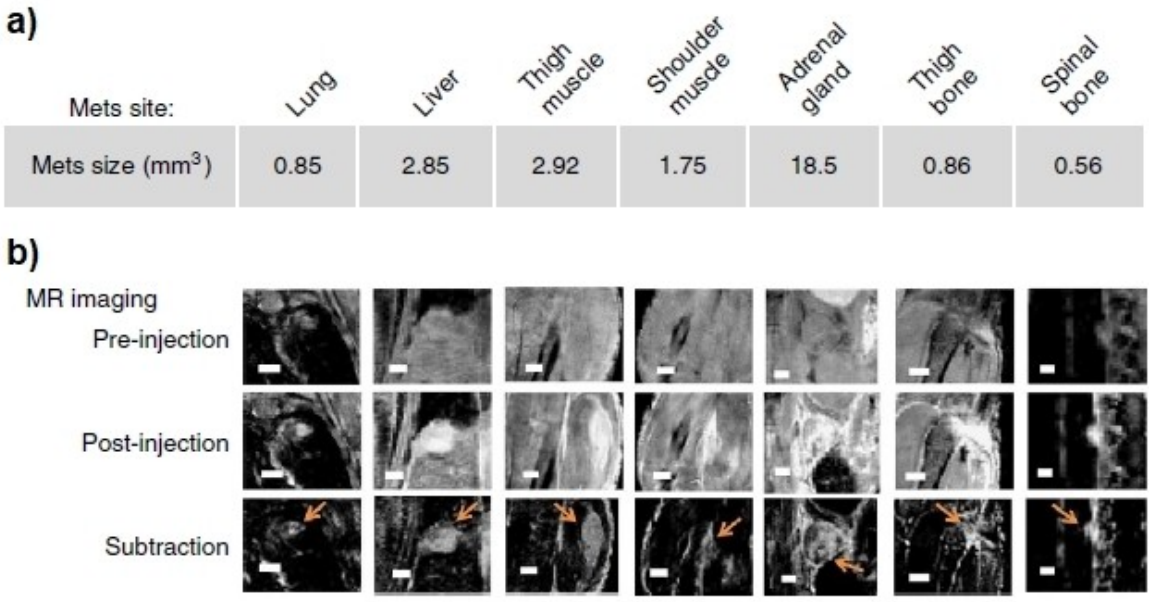

Figure 3. Example of a tripod gadolinium peptide-based MRI contrast agent for fibronectin imaging in metastatic breast tumours. CREKA-Tris(Gd-DOTA)$_3$ enables robust detection of micro-metastases size and location (a). Pre-injection, 25 min post-injection, and subtraction MR images show tumours (arrows). Scale bars = 1 mm (b). *Reproduced from* Ref. .[58] *Copyright (2015), with permission from Springer Nature.*

to a specific MMP or panel of MMPs are retained in the ECM longer than non-binding controls. Given the submicromolar MMP concentrations, very low concentrations of the imaging reporter within the target tissue are expected. Thus, the inhibitor approach is limited to very sensitive imaging techniques as nuclear[77–79] or optical[80] imaging. Despite such limitation, compound P947, composed of a broad spectrum MMP inhibitor conjugated with a single Gd-DOTA derivative, has been shown by in vivo MRI to co-localize with markers of inflammation and MMP activity in atherosclerosis[81] and AAA.[82] However, concerns were raised that these results could be affected by nonspecific accumulation of the probe.[83] High nonspecific signal is indeed a common issue when low molecular weight inhibitors are used, especially hydrophobic ones, irrespective of the imaging modality.[40,84] To increase the MRI sensitivity for the detection of MT1-MMP a pre-targeting approach with a dendrimer carrying 44 Gd-DTPA chelates was developed.[85]

The inhibitor-based approach using high affinity ligands may not be the best for MR imaging of MMPs. An alternative approach is based on cleavable probes, which are MMP substrates rather than inhibitors. Cleavable probes can be considered as analogues of activatable probes such as those frequently used to detect protease activity by OI [reviewed in [86]]. The advantage of the cleavable approach is signal amplification, as many copies of the probes can be processed per unit time. According to the solubility switch approach, short peptide sequences cleavable by MMP-7[87] or MMP-2[88,89] were conjugated to a Gd-DO3AAm chelate through a hydrophobic linker. The fragment released after enzymatic cleavage is more hydrophobic than the parent compound, resulting in greater affinity towards the ECM compartment and increased tissue contrast enhancement. In a reverse approach, a very hydrophobic MMP-2 cleavable peptide labelled with a Gd-DO3AAm complex was shown to have long retention times within the ECM.[90] The cleaved fragment, being hydrophilic, had much faster tissue clearance. The key feature with cleavable probes is that MMP activity modulate the pharmacokinetics of contrast enhancement. However, the tissue pharmacokinetics of both the intact probe and the activated fragment may also depend on tissue properties that are not related to MMP activity, causing uncertainties about the actual MMP activity. A more reliable assessment could be achieved by combining the cleavable probe approach with ratiometry, that enables one to assess the mixing ratio between the intact and cleaved forms of the probe without knowing *a priori* the total concentration of Gd(III). T_2/T_1 ratiometry was applied to assess MMP-2 activity in vitro using a liposome decorated with a cleavable peptide bearing a Gd-DO3AAm chelate.[91] MMP-2 could cleave the peptide exposed on the liposome surface thus releasing Gd(III)-complex as a free, low molecular weight fragment characterized by a major change of the T_2/T_1 ratio. Thus, T_2/T_1 maps could be read as enzyme activity maps. Ratiometry requires high magnetic fields (7T or higher) to ensure a large change of the T_2/T_1 ratio between the intact and the cleaved forms of the probe.

4. Conclusions - Unmet Needs and Future Directions

Key challenges exist in translating molecular MR imaging probes for diagnosing fibrotic diseases in humans:

1) Imaging probes require extensive preclinical safety evaluation before they can be tested in humans.
2) The synthesis of the agent will need to be significantly and safely upscaled to satisfy the higher amount required for humans.
3) The tissue concentration of the ECM proteins and the probe pharmacokinetics may differ in humans.
4) Validation and assessment of the imaging tests' sensitivity, specificity and accuracy requires a ground-truth (e.g., tissue histology) which may not always be available in humans.
5) The repeatability and reproducibility of the imaging test will need to be tested among patients and different vendors' scanners.
6) Safety concerns about GBCA relating to nephrogenic systemic fibrosis and Gd(III) deposition in the brain have been raised recently. Contrast agents based on Mn(II) chelates could be a safer alternative to Gd(III).

Despite these challenges, we anticipate that several probes will successfully be translated into clinical use in the next few years. Multimeric probes carrying multiple Gd-DOTA-like units appear most promising, as they combine higher relaxivities with more favorable pharmacokinetics of signal enhancement.

Acknowledgements

We are grateful for funding to the: (1) British Heart Foundation (PG/10/044/28343, RG/12/1/29262, PG/2019/34897, and RG/20/1/34802); (2) King's BHF Centre for Research Excellence (RE/08/03); (3) Wellcome EPSRC Centre for Medical Engineering (NS/A000049/1); (4) Department of Health via the National Institute for Health Research (NIHR) Cardiovascular Health Technology Cooperative (HTC) and comprehensive Biomedical Research Centre awarded to Guy's & St Thomas' NHS Foundation Trust in partnership with King's College London and King's College Hospital NHS Foundation Trust; (5) EU's H2020 research and innovation program under the grant agreement No. 633937 (SPCCT).

Conflict of Interest

The authors declare no conflict of interest.

Keywords: ECM proteins · fibrosis · molecular imaging · MRI · targeted contrast agents

[1] D. C. Rockey, P. D. Bell, J. A. Hill, *N. Engl. J. Med.* **2015**, *373*, 96.
[2] T. A. Wynn, T. R. Ramalingam, *Nat. Med.* **2012**, *18*, 1028–1040.
[3] B. Piersma, M. K. Hayward, V. M. Weaver, *Biochim. Biophys. Acta Rev. Cancer* **2020**, *1873*, 188356.

[4] S. Gupta, Y. Ge, A. Singh, C. Grani, R. Y. Kwong, *JACC* **2021**, *14*, 2457–2469.
[5] F. Vernuccio, R. Cannella, T. V. Bartolotta, M. Galia, A. Tang, G. Brancatelli, *Eur. Radiol.* **2021**, *5*, 52.
[6] S. B. Montesi, P. Desogere, B. C. Fuchs, P. Caravan, *J. Clin. Invest.* **2019**, *129*, 24–33.
[7] J. K. Mouw, G. Ou, V. M. Weaver, *Nat. Rev. Mol. Cell Biol.* **2014**, *15*, 771–785.
[8] B. S. Brooke, A. Bayes-Genis, D. Y. Li, *Trends Cardiovasc. Med.* **2003**, *13*, 176–181.
[9] S. G. Wise, A. S. Weiss, *Int. J. Biochem. Cell Biol.* **2009**, *41*, 494–497.
[10] E. A. Lenselink, *Int. Wound J.* **2015**, *12*, 313–316.
[11] J. Patten, K. Wang, *Adv. Drug Delivery Rev.* **2021**, *170*, 353–368.
[12] H. Ghura, M. Keimer, A. von Au, N. Hackl, V. Klemis, I. A. Nakchbandi, *Neoplasia.* **2021**, *23*, 837–850.
[13] M. W. Mosesson, *J. Thromb. Haemostasis* **2005**, *3*, 1894–1904.
[14] M. L. James, S. S. Gambhir, *Physiol. Rev.* **2012**, *92*, 897–965.
[15] P. Caravan, C. T. Farrar, L. Frullano, R. Uppal, *Contrast Media Mol. Imaging.* **2009**, *4*, 89–100.
[16] S. Aime, M. Botta, E. Terreno, *Adv. Inorg. Chem.* **2005**, *57*, 173–237.
[17] S. Aime, M. Botta, D. Esteban-Gómez, C. Platas-Iglesias, *Mol. Phys.* **2019**, *117*, 898–909.
[18] A. Merbach, L. Lothar, E. Tóth, *The Chemistry of Contrast Agents in Medical Magnetic Resonance 2nd edition, John Wiley & Sons publication.* **2013**.
[19] D. Ma, V. Gulani, N. Seiberlich, K. Liu, J. L. Sunshine, J. L. Duerk, M. A. Griswold, *Nature.* **2013**, *495*, 187–192.
[20] C. E. Anderson, S. B. Donnola, Y. Jiang, J. Batesole, R. Darrah, M. L. Drumm, S. M. Brady-Kalnay, N. F. Steinmetz, X. Yu, M. A. Griswold, C. A. Flask, *Sci. Rep.* **2017**, *7*, 8431.
[21] Y. Gao, Y. Chen, D. Ma, Y. Jiang, K. A. Herrmann, J. A. Vincent, K. M. Dell, M. L. Drumm, S. M. Brady-Kalnay, M. A. Griswold, C. A. Flask, L. Lu, *NMR Biomed.* **2015**, *28*, 384–394.
[22] D. Onthank, P. Yalamanchili, R. Cesati, J. Lazewatsky, M. Azure, M. Hayes, M. Kavosi, K. Spencer, D. Sousa, E. Wexler, M. Lamoy, T. Harris, C. Hu, R. Jones, G. Dwyer, D. Casebier, S. Robinson, *Circulation.* **2007**, *116*, II 411–412.
[23] M. R. Makowski, A. J. Wiethoff, U. Blume, F. Cuello, A. Warley, C. H. Jansen, E. Nagel, R. Razavi, D. C. Onthank, R. R. Cesati, M. S. Marber, T. Schaeffter, A. Smith, S. P. Robinson, R. M. Botnar, *Nat. Med.* **2011**, *17*, 383–388.
[24] R. M. Botnar, A. J. Wiethoff, U. Ebersberger, S. Lacerda, U. Blume, A. Warley, C. H. Jansen, D. C. Onthank, R. R. Cesati, R. Razavi, M. S. Marber, B. Hamm, T. Schaeffter, S. P. Robinson, M. R. Makowski, *Circ. Cardiovasc. Imaging.* **2014**, *7*, 679–689.
[25] A. Phinikaridou, M. E. Andia, A. Indermuehle, D. C. Onthank, R. R. Cesati, A. Smith, S. P. Robinson, P. Saha, R. M. Botnar, *Radiology.* **2014**, *271*, 390–399.
[26] M. R. Makowski, A. Preissel, C. von Bary, A. Warley, S. Schachoff, A. Keithan, R. R. Cesati, D. C. Onthank, M. Schwaiger, S. P. Robinson, R. M. Botnar, *Invest. Radiol.* **2012**, *47*, 438–444.
[27] C. von Bary, M. Makowski, A. Preissel, A. Keithahn, A. Warley, E. Spuentrup, A. Buecker, J. Lazewatsky, R. Cesati, D. Onthank, N. Schickl, S. Schachoff, J. Hausleiter, A. Schomig, M. Schwaiger, S. Robinson, R. Botnar, *Circ. Cardiovasc. Imaging.* **2011**, *4*, 147–155.
[28] M. Wildgruber, I. Bielicki, M. Aichler, K. Kosanke, A. Feuchtinger, M. Settles, D. C. Onthank, R. R. Cesati, S. P. Robinson, A. M. Huber, E. J. Rummeny, A. K. Walch, R. M. Botnar, *Circ. Cardiovasc. Imaging.* **2014**, *7*, 321–329.
[29] A. Protti, B. Lavin, X. Dong, S. Lorrio, S. Robinson, D. Onthank, A. M. Shah, R. M. Botnar, *J. Am. Heart Assoc.* **2015**, *4*, e001851.
[30] Q. Sun, M. Baues, B. M. Klinkhammer, J. Ehling, S. Djudjaj, N. I. Drude, C. Daniel, K. Amann, R. Kramann, H. Kim, J. Saez-Rodriguez, R. Weiskirchen, D. C. Onthank, R. M. Botnar, F. Kiessling, J. Floege, T. Lammers, P. Boor, *Sci. Transl. Med.* **2019**, *11*.
[31] J. Ehling, M. Bartneck, V. Fech, B. Butzbach, R. Cesati, R. Botnar, T. Lammers, F. Tacke, *Hepatology.* **2013**, *58*, 1517–1518.
[32] A. Phinikaridou, S. Lacerda, B. Lavin, M. E. Andia, A. Smith, P. Saha, R. M. Botnar, *Circ. Cardiovasc. Imaging.* **2018**, *11*.
[33] B. Lavin, S. Lacerda, M. E. Andia, S. Lorrio, R. Bakewell, A. Smith, I. Rashid, R. M. Botnar, A. Phinikaridou, *Cardiovasc. Res.* **2020**, *116*, 995–1005.
[34] F. Capuana, A. Phinikaridou, R. Stefania, S. Padovan, B. Lavin, S. Lacerda, E. Almouazen, Y. Chevalier, L. Heinrich-Balard, R. M. Botnar, S. Aime, G. Digilio, *J. Med. Chem.* **2021**, *64*, 15250–15261.
[35] A. Krettek, G. K. Sukhova, P. Libby, *Arterioscler. Thromb. Vasc. Biol.* **2003**, *23*, 582–587.
[36] P. Caravan, B. Das, S. Dumas, F. H. Epstein, P. A. Helm, V. Jacques, S. Koerner, A. Kolodziej, L. Shen, W. C. Sun, Z. Zhang, *Angew. Chem. Int. Ed. Engl.* **2007**, *46*, 8171–8173.
[37] B. C. Fuchs, H. Wang, Y. Yang, L. Wei, M. Polasek, D. T. Schuhle, G. Y. Lauwers, A. Parkar, A. J. Sinskey, K. K. Tanabe, P. Caravan, *J. Hepatol.* **2013**, *59*, 992–998.
[38] M. Polasek, B. C. Fuchs, R. Uppal, D. T. Schuhle, J. K. Alford, G. S. Loving, S. Yamada, L. Wei, G. Y. Lauwers, A. R. Guimaraes, K. K. Tanabe, P. Caravan, *J. Hepatol.* **2012**, *57*, 549–555.
[39] P. Caravan, Y. Yang, R. Zachariah, A. Schmitt, M. Mino-Kenudson, H. H. Chen, D. E. Sosnovik, G. Dai, B. C. Fuchs, M. Lanuti, *Am. J. Respir. Cell Mol. Biol.* **2013**, *49*, 1120–1126.
[40] A. P. Murphy, E. Greally, D. O'Hogain, A. Blamire, P. Caravan, V. Straub, *Magn. Reson. Med.* **2019**, *81*, 2728–2735.
[41] M. Polasek, Y. Yang, D. T. Schuhle, M. A. Yaseen, Y. R. Kim, Y. S. Sung, A. R. Guimaraes, P. Caravan, *Sci. Rep.* **2017**, *7*, 8114.
[42] C. T. Farrar, D. K. DePeralta, H. Day, T. A. Rietz, L. Wei, G. Y. Lauwers, B. Keil, A. Subramaniam, A. J. Sinskey, K. K. Tanabe, B. C. Fuchs, P. Caravan, *J. Hepatol.* **2015**, *63*, 689–696.
[43] C. T. Farrar, E. M. Gale, R. Kennan, I. Ramsay, R. Masia, G. Arora, K. Looby, L. Wei, J. Kalpathy-Cramer, M. M. Bunzel, C. Zhang, Y. Zhu, T. E. Akiyama, M. Klimas, S. Pinto, H. Diyabalanage, K. K. Tanabe, V. Humblet, B. C. Fuchs, P. Caravan, *Radiology.* **2018**, *287*, 581–589.
[44] P. Desogere, L. F. Tapias, L. P. Hariri, N. J. Rotile, T. A. Rietz, C. K. Probst, F. Blasi, H. Day, M. Mino-Kenudson, P. Weinreb, S. M. Violette, B. C. Fuchs, A. M. Tager, M. Lanuti, P. Caravan, *Sci. Transl. Med.* **2017**, *9*.
[45] S. Xue, J. Qiao, J. Jiang, K. Hubbard, N. White, L. Wei, S. Li, Z. R. Liu, J. J. Yang, *Med. Res. Rev.* **2014**, *34*, 1070–1099.
[46] M. Salarian, R. C. Turaga, S. Xue, M. Nezafati, K. Hekmatyar, J. Qiao, Y. Zhang, S. Tan, O. Y. Ibhagui, Y. Hai, J. Li, R. Mukkavilli, M. Sharma, P. Mittal, X. Min, S. Keilholz, L. Yu, G. Qin, A. B. Farris, Z. R. Liu, J. J. Yang, *Nat. Commun.* **2019**, *10*, 4777.
[47] W. Chen, D. P. Cormode, Y. Vengrenyuk, B. Herranz, J. E. Feig, A. Klink, W. J. Mulder, E. A. Fisher, Z. A. Fayad, *JACC* **2013**, *6*, 373–384.
[48] Y. Zong, Y. Xu, X. Liang, D. R. Keene, A. Hook, S. Gurusiddappa, M. Hook, S. V. Narayana, *EMBO J.* **2005**, *24*, 4224–4236.
[49] A. Klink, J. Heynens, B. Herranz, M. E. Lobatto, T. Arias, H. M. Sanders, G. J. Strijkers, M. Merkx, K. Nicolay, V. Fuster, A. Tedgui, Z. Mallat, W. J. Mulder, Z. A. Fayad, *J. Am. Coll. Cardiol.* **2011**, *58*, 2522–2530.
[50] G. S. van Bochove, H. M. H. F. Sanders, M. de Smet, H. M. Keizer, W. J. M. Mulder, R. Krams, G. J. Strijkers, K. Nicolay, *Eur. J. Inorg. Chem.* **2012**, *2012*, 2115–2125.
[51] H. H. Chen, P. A. Waghorn, L. Wei, L. F. Tapias, D. T. Schuhle, N. J. Rotile, C. M. Jones, R. J. Looby, G. Zhao, J. M. Elliott, C. K. Probst, M. Mino-Kenudson, G. Y. Lauwers, A. M. Tager, K. K. Tanabe, M. Lanuti, B. C. Fuchs, P. Caravan, *JCI. Insight.* **2017**, *2*.
[52] E. A. Akam, E. Abston, N. J. Rotile, H. R. Slattery, I. Y. Zhou, M. Lanuti, P. Caravan, *Chem. Sci.* **2020**, *11*, 224–231.
[53] P. A. Waghorn, C. M. Jones, N. J. Rotile, S. K. Koerner, D. S. Ferreira, H. H. Chen, C. K. Probst, A. M. Tager, P. Caravan, *Angew. Chem. Int. Ed. Engl.* **2017**, *56*, 9825–9828.
[54] A. Koudrina, E. M. McConnell, J. A. Zurakowski, G. O. Cron, S. Chen, E. C. Tsai, M. C. DeRosa, *ACS Appl. Mater. Interfaces* **2021**, *13*, 9412–9424.
[55] F. Ye, X. Wu, E. K. Jeong, Z. Jia, T. Yang, D. Parker, Z. R. Lu, *Bioconjugate Chem.* **2008**, *19*, 2300–2303.
[56] M. Tan, S. M. Burden-Gulley, W. Li, X. Wu, D. Lindner, S. M. Brady-Kalnay, V. Gulani, Z. R. Lu, *Pharm. Res.* **2012**, *29*, 953–960.
[57] X. Wu, G. Yu, D. Lindner, S. M. Brady-Kalnay, Q. Zhang, Z. R. Lu, *Am. J. Nucl. Med. Mol. Imaging* **2014**, *4*, 525–536.
[58] Z. Zhou, M. Qutaish, Z. Han, R. M. Schur, Y. Liu, D. L. Wilson, Z. R. Lu, *Nat. Commun.* **2015**, *6*, 7984.
[59] S. Aime, L. Calabi, C. Cavallotti, E. Gianolio, G. B. Giovenzana, P. Losi, A. Maiocchi, G. Palmisano, M. Sisti, *Inorg. Chem.* **2004**, *43*, 7588–7590.
[60] A. Pagoto, M. Tripepi, R. Stefania, S. Lanzardo, D. Livio Longo, F. Garello, F. Porpiglia, M. Manfredi, S. Aime, E. Terreno, *Magn. Reson. Med.* **2019**, *81*, 1935–1946.
[61] N. R. Ayat, A. Vaidya, G. A. Yeung, M. N. Buford, R. C. Hall, P. L. Qiao, X. Yu, Z. R. Lu, *Front. Oncol.* **2019**, *9*, 1351.
[62] P. Qiao, N. R. Ayat, A. Vaidya, S. Gao, W. Sun, S. Chou, Z. Han, H. Gilmore, J. M. Winter, Z. R. Lu, *Front. Oncol.* **2020**, *10*, 586727.
[63] P. L. Qiao, M. Gargesha, Y. Liu, V. E. A. Laney, R. C. Hall, A. M. Vaidya, H. Gilmore, K. Gawelek, B. B. Scott, D. Roy, D. L. Wilson, Z. R. Lu, *Magn. Reson. Imaging.* **2022**, *86*, 37–45.

[64] M. Yu, C. A. Ortega, K. Si, R. Molinaro, F. J. Schoen, R. F. C. Leitao, X. Xu, M. Mahmoudi, S. Ahn, J. Liu, P. E. Saw, I. H. Lee, M. M. B. Brayner, A. Lotfi, J. Shi, P. Libby, S. Jon, O. C. Farokhzad, *Theranostics* **2018**, *8*, 6008–6024.
[65] R. M. Botnar, A. S. Perez, S. Witte, A. J. Wiethoff, J. Laredo, J. Hamilton, W. Quist, E. C. Parsons, Jr., A. Vaidya, A. Kolodziej, J. A. Barrett, P. B. Graham, R. M. Weisskoff, W. J. Manning, M. T. Johnstone, *Circulation.* **2004**, *109*, 2023–2029.
[66] K. Overoye-Chan, S. Koerner, R. J. Looby, A. F. Kolodziej, S. G. Zech, Q. Deng, J. M. Chasse, T. J. McMurry, P. Caravan, *J. Am. Chem. Soc.* **2008**, *130*, 6025–6039.
[67] M. E. Andia, P. Saha, J. Jenkins, B. Modarai, A. J. Wiethoff, A. Phinikaridou, S. P. Grover, A. S. Patel, T. Schaeffter, A. Smith, R. M. Botnar, *Arterioscler. Thromb. Vasc. Biol.* **2014**, *34*, 1193–1198.
[68] M. R. Makowski, S. C. Forbes, U. Blume, A. Warley, C. H. Jansen, A. Schuster, A. J. Wiethoff, R. M. Botnar, *Atherosclerosis* **2012**, *222*, 43–49.
[69] E. Spuentrup, R. Botnar, A. Binder, M. Katoh, C. Spuntrup, *Clin. Neuroradiol.* **2021**, *31*, 925–931.
[70] E. Spuentrup, R. M. Botnar, A. J. Wiethoff, T. Ibrahim, S. Kelle, M. Katoh, M. Ozgun, E. Nagel, J. Vymazal, P. B. Graham, R. W. Gunther, D. Maintz, *Eur. Radiol.* **2008**, *18*, 1995–2005.
[71] M. Tripepi, F. Capuana, E. Gianolio, F. V. C. Kock, A. Pagoto, R. Stefania, G. Digilio, S. Aime, *Bioconjugate Chem.* **2018**, *29*, 1428–1437.
[72] S. Shuvaev, E. Akam, P. Caravan, *Invest. Radiol.* **2021**, *56*, 20–34.
[73] F. Rodriguez-Pascual, T. Rosell-Garcia, *Anal. Biochem.* **2022**, *639*, 114508.
[74] F. Casalini, L. Fugazza, G. Esposito, C. Cabella, C. Brioschi, A. Cordaro, L. D'Angeli, A. Bartoli, A. M. Filannino, C. V. Gringeri, D. L. Longo, V. Muzio, E. Nuti, E. Orlandini, G. Figlia, A. Quattrini, L. Tei, G. Digilio, A. Rossello, A. Maiocchi, *J. Med. Chem.* **2013**, *56*, 2676–2689.
[75] Z. S. Galis, J. J. Khatri, *Circ. Res.* **2002**, *90*, 251–262.
[76] M. Giannandrea, W. C. Parks, *Dis. Models Mech.* **2014**, *7*, 193–203.
[77] S. Hermann, A. Starsichova, B. Waschkau, M. Kuhlmann, C. Wenning, O. Schober, M. Schafers, *J. Nucl. Cardiol.* **2012**, *19*, 609–617.
[78] L. Rangasamy, B. D. Geronimo, I. Ortin, C. Coderch, J. M. Zapico, A. Ramos, B. de Pascual-Teresa, *Molecules* **2019**, *24*.
[79] N. Chaher, R. Hajhosseiny, A. Phinikaridou, R. M. Botnar, *Appl. Sci.* **2020**, *10*, 4001.
[80] R. Seifert, M. T. Kuhlmann, S. Eligehausen, F. Kiefer, S. Hermann, M. Schafers, *PLoS One.* **2018**, *13*, e0204305.
[81] F. Hyafil, E. Vucic, J. C. Cornily, R. Sharma, V. Amirbekian, F. Blackwell, E. Lancelot, C. Corot, V. Fuster, Z. S. Galis, L. J. Feldman, Z. A. Fayad, *Eur. Heart J.* **2011**, *32*, 1561–1571.
[82] R. Bazeli, M. Coutard, B. D. Duport, E. Lancelot, C. Corot, J. P. Laissy, D. Letourneur, J. B. Michel, J. M. Serfaty, *Invest. Radiol.* **2010**, *45*, 662–668.
[83] R. Lebel, M. Lepage, *Contrast Media Mol. Imaging* **2014**, *9*, 187–210.
[84] G. Digilio, T. Tuccinardi, F. Casalini, C. Cassino, D. M. Dias, C. F. Geraldes, V. Catanzaro, A. Maiocchi, A. Rossello, *Eur. J. Med. Chem.* **2014**, *79*, 13–23.
[85] K. Sano, T. Temma, T. Azuma, R. Nakai, M. Narazaki, Y. Kuge, H. Saji, *Mol. Imaging Biol.* **2011**, *13*, 1196–1203.
[86] E. R. H. Walter, S. M. Cooper, J. J. Boyle, N. J. Long, *Dalton Trans.* **2021**, *50*, 14486–14497.
[87] M. Lepage, W. C. Dow, M. Melchior, Y. You, B. Fingleton, C. C. Quarles, C. Pepin, J. C. Gore, L. M. Matrisian, J. O. McIntyre, *Mol. Imaging* **2007**, *6*, 393–403.
[88] B. Jastrzebska, R. Lebel, H. Therriault, J. O. McIntyre, E. Escher, B. Guerin, B. Paquette, W. A. Neugebauer, M. Lepage, *J. Med. Chem.* **2009**, *52*, 1576–1581.
[89] R. Lebel, B. Jastrzebska, H. Therriault, M. M. Cournoyer, J. O. McIntyre, E. Escher, W. Neugebauer, B. Paquette, M. Lepage, *Magn. Reson. Med.* **2008**, *60*, 1056–1065.
[90] C. V. Gringeri, V. Menchise, S. Rizzitelli, E. Cittadino, V. Catanzaro, G. Dati, L. Chaabane, G. Digilio, S. Aime, *Contrast Media Mol. Imaging* **2012**, *7*, 175–184.
[91] V. Catanzaro, C. V. Gringeri, V. Menchise, S. Padovan, C. Boffa, W. Dastru, L. Chaabane, G. Digilio, S. Aime, *Angew. Chem. Int. Ed. Engl.* **2013**, *52*, 3926–3930.

Manuscript received: June 3, 2022
Revised manuscript received: August 22, 2022
Accepted manuscript online: August 25, 2022
Version of record online: ■■, ■■■

CONCEPT

Gadolinium based MRI probes targeted to ECM components, either proteins or enzymes, hold promise for accurate molecular characterization and staging of fibrotic diseases in vivo. Non-covalent binding probes (1), reactive probes (2), and enzyme-responsive probes (3) are discussed.

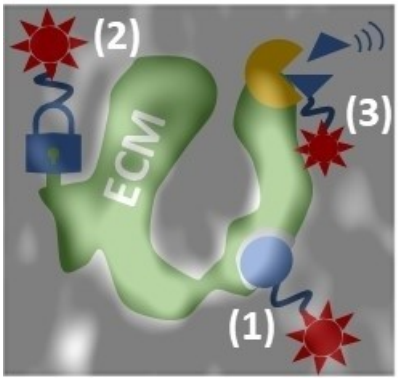

*Dr. G. Digilio, Dr. S. Lacerda, Dr. B. Lavin Plaza, Dr. A. Phinikaridou**

1 – 10

Extracellular Matrix Targeted MRI Probes